POLITECNICO DI TORINO
Repository ISTITUZIONALE

Investigation on the Susceptibility to RFI of High-Voltage Current Sensors

Original
Investigation on the Susceptibility to RFI of High-Voltage Current Sensors / Fiori, F.. - STAMPA. - (2025), pp. 854-859. (International Symposium on Electromagnetic Compatibility (EMC Europe) Parigi (Fra) 1-5 September 2025) [10.1109/EMCEurope61644.2025.11176264].

Availability:
This version is available at: 11583/3003260 since: 2025-09-23T12:10:43Z

Publisher:
IEEE

Published
DOI:10.1109/EMCEurope61644.2025.11176264

Terms of use:

This article is made available under terms and conditions as specified in the corresponding bibliographic description in the repository

Publisher copyright
IEEE postprint/Author's Accepted Manuscript

©2025 IEEE. Personal use of this material is permitted. Permission from IEEE must be obtained for all other uses, in any current or future media, including reprinting/republishing this material for advertising or promotional purposes, creating new collecting works, for resale or lists, or reuse of any copyrighted component of this work in other works.

(Article begins on next page)

19 November 2026

Investigation on the Susceptibility to RFI of High-Voltage Current Sensors

Franco Fiori
MicroEMC Group, Politecnico di Torino, Italy
franco.fiori@polito.it

***Abstract*— Current sensors inserted in the cables connecting electric drives to power loads are likely exposed to the radio frequency interference (RFI) collected by cables, which behave like unintended antennas. This paper investigates the susceptibility to the RFI of such components referring to the bulk current injection (BCI) test method, which is used at the module level, and to the direct power injection (DPI) test, which applies at the component level. A method to evaluate the RF power level to be applied in the DPI test at the inputs of a current sensor to allow an electronic module comprising that device to pass the BCI test is proposed.**

***Keywords*— Current sensor amplifiers, RF interference, Susceptibility to RFI, RFI rectification, Bulk Current Injection, Direct Power Injection, filter design.**

I. Introduction

Power inverters driving electric motors are usually equipped with circuits that monitor the load currents with the purpose of controlling the load as well as to protect the system from operational or accidental failures. Depending on the current magnitude, on the dynamic range and on the bandwidth needed to control the electric motor effectively or to react to failures, different solutions can be put in place [1], [2]. A common approach consists of a current transformer properly loaded and followed by an amplifier. Once calibrated, the output voltage is proportional to the current flowing in the power cable. Beside the galvanic isolation, this solution can be used over a wide sensing range (up to several kA) with accuracy of about 2-3% but limited bandwidth (below 100 kHz). The limitations due to the current transformer can be addressed using a coreless one, meaning a Rogowski coil. Indeed, it extends both the current range (up to MA) and the sensor bandwidth (up to 1 MHz) with almost no penalty on accuracy. Usually, Rogowsky coils are bulky even if, in recent years, the integration in printed circuit boards (PCBs) has reduced their size significantly [3]. An alternative to current transformers consists in sensing the magnetic field related to the current to be measured. This is done by placing a Hall-effect sensor in the close proximity of the conductor carrying the current to be measured. Usually, this approach works well for currents in the Ampere range, featuring accuracy of about 1-2% and bandwidth below 100 kHz. Another popular solution consists in sensing the voltage drop across a shunt resistor, which is inserted in the current path, purposely. The isolation from the power cable is lost, power losses increases (because of the shunt resistor) but the circuit can easily sense DC currents and reach out higher accuracy

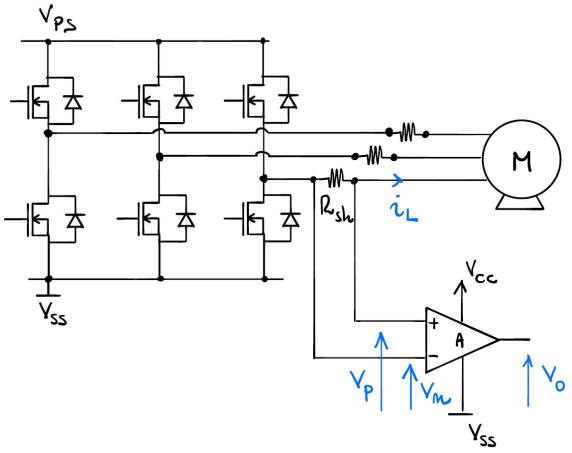


Fig. 1. Simplified schematic view of a three-phase power inverter comprising a not isolated HV current sensor.

levels. Furthermore, the sensor bandwidth can extend to the MHz range.

In recent years, isolated current sensors based on the shunt resistor approach have been developed. The analog front-end is connected to the power cable, meaning to the high-voltage domain. It is made up of a delta-sigma modulator, which outputs are transferred to the low-voltage domain circuits, thus to the output, through capacitive couplings. The bandwidth of such isolated current sensors is usually limited to tens kHz [4].

This paper focuses on not isolated current sensors based on shunt resistors featuring a common mode input range exceeding the power supply one. This allows for sensing the load current in circuits like that shown in Fig.1, where a two-level three-legs power inverter drives an electric motor. A shunt resistor connected to a HV current sensor amplifier for each line is included (only one is shown in Fig.1). Such amplifiers sense the differential input voltage, meaning the voltage drop across the shunt resistors while rejecting the common mode input voltage, i.e., the PWM switching voltage driving the load. Furthermore, being directly connected to the power cable, such current sensors are also exposed to the radio frequency interference (RFI) collected by the cables, which behave like unintended receiving antennas. Such disturbances can be rectified by the transistors composing the current sensor resulting in base band signals affecting the nominal ones. As a result, RF disturbances can lead to unexpected operating failures. To avoid these, electronic modules dealing with safety critical functions, like power

inverters for automotive applications, are requested to comply with stringent immunity standard before being commercialized [5]. The susceptibility to RFI of current sensors has been already investigated in previous works. In [6], the susceptibility to RFI of a Hall-effect current sensor was investigated at the module and at the device level performing bulk current injection (BCI) tests and direct power injection (DPI) tests, respectively. Despite the galvanic isolation from the power cable, the sensor showed high susceptibility to the electric field generated by the current injected in the cable harness. In [7] the immunity of an integrated current sensor based on shunt resistance was investigated. The high-side current sensing based on a feedback opamp was considered. It was found that the RFI applied to the current sensor inputs is demodulated by the OpAmp input stage. Furthermore, the paper shows that the RFI-induced offset does not change if the continuous-time OpAmp is replaced by a chopper one. Over the years, the susceptibility of more complex integrated circuits comprising current sensors was investigated [8], [9], and novel solutions to increase their immunity to RFI have been proposed [10], [11], [12].

Unexpectedly, the susceptibility to RFI of in-line current sensors based on shunt resistor like that shown in Fig. 1 has not been investigated yet. This paper focuses on this topic, providing experimental evidence of the susceptibility issues through measurement results obtained from tests carried out at module and at component level. The power level to be applied to the current sensor inputs in the DPI tests to achieve the immunity level required at the module with the BCI test is evaluated, and a method to increase the immunity of a susceptible current sensor by filtering its input signals is presented.

The paper is organized as follows. Section II presents the main features of in-line not isolated current sensors. Section III shows the test board and the test setup used in this work to perform the DPI and the BCI tests on such components. The measurement results of the BCI test are presented and a method to evaluate the magnitude of the RF power the current sensor should be immune to in the DPI test to pass the BCI one is proposed in Section IV. The design of the filter to be inserted between the shunt resistor and the amplifier input to achieve the immunity to the RFI is presented in Section V, and some concluding remarks are drawn in Section VI.

II. In-line Not Isolated Current Sensors

In-line current sensors are differential amplifiers whose output voltage is proportional to the differential input one, which drops across a shunt resistor because of the load current flowing through it. The output voltage can be expressed as

$$V_{\rm o} = AR_{\rm sh}i_{\rm L}, \tag{1}$$

where $V_{\rm o}$ is the amplifier output voltage, A is the voltage gain (usually it is set by the silicon maker and cannot be changed by the user), $R_{\rm sh}$ is the shunt resistance, $i_{\rm L}$ is the load current. In power applications like that shown in Fig. 1 the amplifier input voltages can easily exceed the power-supply voltage

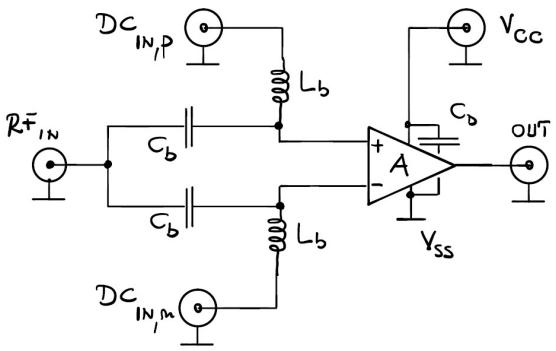


Fig. 2. Schematic view of the test board used to perform DPI immunity tests on the current sensor amplifier.

range, meaning $V_{\rm cm} < V_{\rm ss}$ or $V_{\rm cm} > V_{\rm cc}$, where $V_{\rm ss}$ is the negative power supply and $V_{\rm cc}$ is the positive one. $V_{\rm cm}$ is the common mode input voltage, which is defined as

$$V_{\rm cm} = \frac{V_{\rm p} + V_{\rm m}}{2}, \tag{2}$$

where $V_{\rm p}$ and $V_{\rm m}$ are the positive and negative input voltages, respectively. In practice, being $V_{\rm p} \simeq V_{\rm m}$, $V_{\rm cm}$ is the output voltage of a switching leg (see Fig. 1). This means that the amplifier should be able to reject a fast switching common-mode input voltage while amplifying the differential one $V_{\rm d} = V_{\rm p} - V_{\rm m}$.

Usually, in-line current sense amplifiers show input range $-4V < V_{\rm cm} < 80V$, DC common mode rejection ratio $\mathrm{CMRR_{DC}} \simeq 130\ dB$ and AC $\mathrm{CMRR_{AC}} \simeq 90\ dB$ [13]. In real applications, the amplifier output voltage is provided to the analog input of a microcontroller, i.e., the input of its analog-to-digital converter (ADC), which usually shows an effective number of bit in the range $8 < \mathrm{ENOB} < 12$. Therefore, if the ADC input range is $V_{\rm ref} = 3V$, the effective resolution is in the range $700\mu V < \mathrm{LSB} < 12mV$. Finally, being the amplifier voltage gain in the range $20 < A < 100$, and wanting to keep the amplifier output within 1-LSB, the equivalent input offset voltage should be in the tens μV range. For this reason, current sense amplifiers are characterized by low input offset voltage (tens μV), which is usually obtained referring to chopper or switched capacitor architectures. About the shunt resistance, its value is selected on the basis of the current range to be covered, and with the aim to reduce its power dissipation as much as possible. Usually, it takes values from a few $m\Omega$ to a few hundred $m\Omega$. Being used in switching circuits, also its self inductance is kept as low as possible and usually it takes values $L_{\rm sh} < 10nH$. In practice, the amplifier inputs are almost shorted by the shunt resistance, therefore, wanting to evaluate the susceptibility to RFI of such an amplifier, the interference should be applied to both inputs, simultaneously. To do that, a test board compliant to IEC 62132 [14] was designed and prototyped. The test board schematic view is shown in Fig. 2. It comprises a current sensor amplifier featuring voltage gain $A = 20$, the bias tees needed to provide the input bias voltage $V_{\rm p}$ as well as to apply the RFI to the amplifier inputs. The direct power

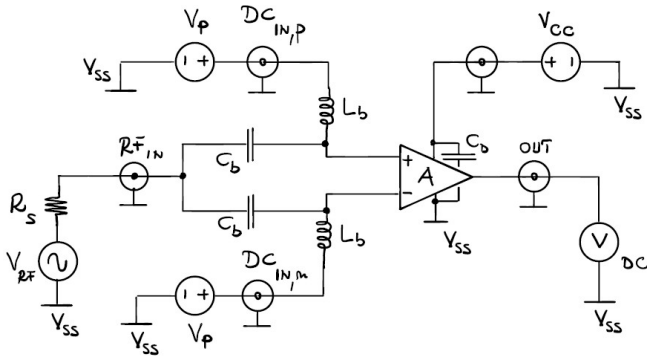


Fig. 3. Schematic view of the DPI test bench.

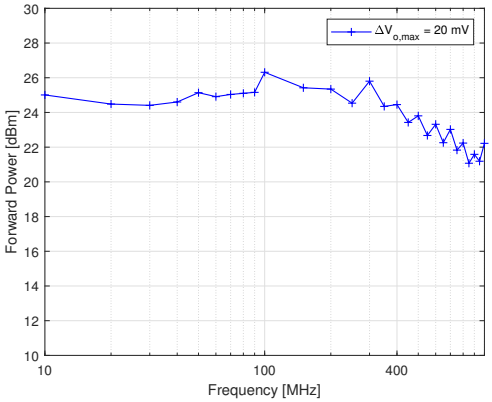


Fig. 4. DPI test results obtained with the common mode injection of the interference (test setup shown in Fig. 3) and maximum output offset voltage $\Delta V_{\mathrm{o,max}} = 20\ mV$.

injection (DPI) test was carried out referring to the test bench shown in Fig. 3, which comply to IEC 62132-4. The DC power supply provided to the amplifier was $V_{\mathrm{cc}} = 3.3V$, the DC input voltage was $V_{\mathrm{p}} = 0V$. The output voltage was monitored by a DC voltmeter while a continuous wave (CW) interference was applied to the amplifier inputs through the bias tees (RF_{in}). The source of interference is shown in Fig. 3 by the real voltage source ($V_{\mathrm{RF}} - R_{\mathrm{S}}$). In the test, the magnitude of the interference was increased as long as the susceptibility criterion, which was set a-priori, was violated. The offset voltage induced by the RFI should be always lower than $\Delta V_{\mathrm{o,max}} = 20\ mV$. This value deals with maximum error affecting the acquired current level (Δi_{L}) that can be accepted at the application level. In our case, $\Delta i_{\mathrm{L}} = 100\ mA$, therefore for $R_{\mathrm{sh}} = 10\ m\Omega$ and $A = 20$ from (1) maximum output offset voltage mentioned above is obtained. The measurement results of the DPI test are shown in Fig. 4.

III. BCI Immunity Test

Aiming to check the immunity to RFI of the same device but included in a real application, a test board comprising a power stage, an in-line current sensor and a microcontroller acquiring the current sensor output voltage was designed and prototyped. A schematic view of such a test board is shown in Fig. 5. The power section comprises a H-bridge, a DC-link capacitor (C_{DC}) and a power supply EMI filter including the C_{y} capacitors. Furthermore, one of the H-bridge outputs hosts

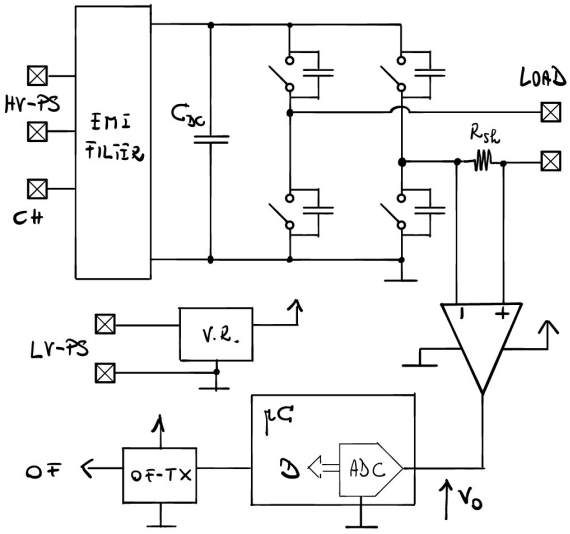


Fig. 5. Simplified schematic view of the application board designed to evaluate the immunity of HV current sensor to the RFI injected in the cable harness.

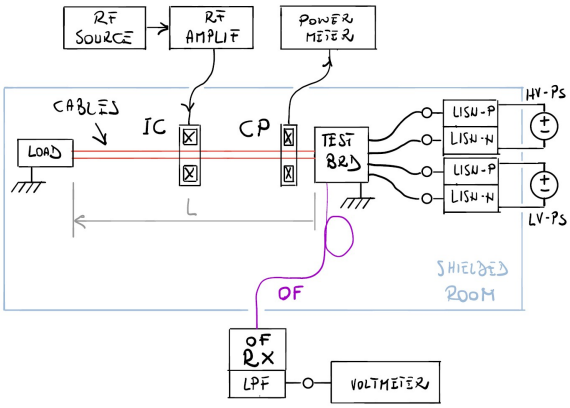


Fig. 6. Schematic view of the BCI test bench.

a shunt resistor R_{sh}, which is connected to the inputs of the current sensor amplifier. The output (V_{o}) is provided to the ADC of a microcontroller, which is programmed to modulate the duty cycle of a digital output according to V_{o}. Such a digital output drives an optic fiber transmitter (OF-TX in Fig. 5). About the power section, instead of the transistors and the circuits needed to make them switch, mechanical switches in parallel to $C_{\mathrm{DS}} = 1\ nF$ capacitors were included. This avoids the rectification of the RFI in nonlinear circuits other than the current sensor amplifier, thus avoiding the superposition of failures originating from different devices [16].

Overall, the test board shows a connector to supply the *power section* (HV-PS), the terminal (CH) to connect the C_{y} capacitors to the chassis, a connector (LV-PS) to supply the *signal section*, meaning the microcontroller, the current sensor and the optic fiber transmitter (OF-TX), and the terminals (LOAD) to connect the power load. Such a test board was designed and prototyped then included in the test bench shown in Fig. 6 with the aim to perform BCI tests compliant to [5]. The test board outputs are connected to an inductive load by two cables of length $L = 1m$. The *power section*

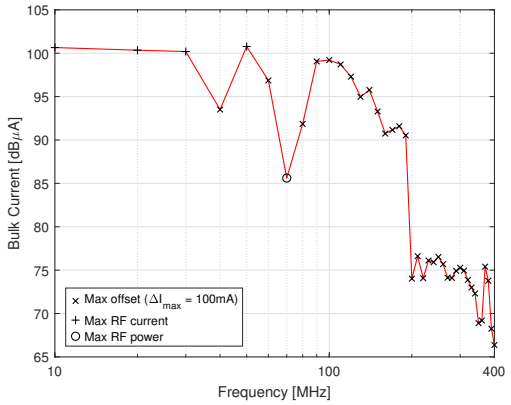


Fig. 7. BCI test results. Crosses (x) point out that the susceptibility criterion $\Delta V_{\mathrm{o,max}} = 20\ mV$ was exceeded, circles (o) that the maximum bulk current level of $I_{\mathrm{RF-max}} = 100\ dB\mu A$ was reached without exceeding $\Delta V_{\mathrm{o,max}}$, crosses (+) that the maximum available power level of the RF amplifier $P_{\mathrm{RF-max}} = 100\ W$ was reached without exceeding $\Delta V_{\mathrm{o,max}}$.

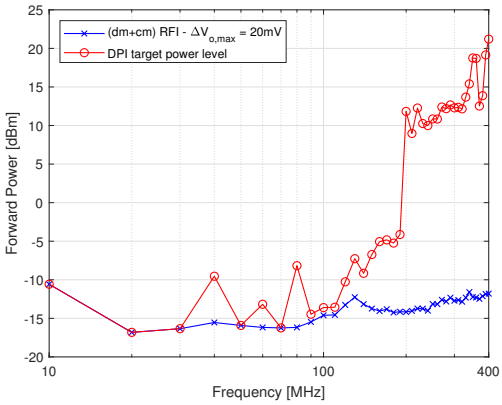


Fig. 8. DPI test results obtained with the common mode and the differential mode applied to the inputs (see the test setup shown in Fig. 3) and maximum output offset voltage $\Delta V_{\mathrm{o,max}} = 20\ mV$ (Blue crosses). DPI target power level to comply to BCI immunity test specification versus frequency (red circles).

is supplied by a $48V$ DC voltage source through two Line Impedance Stabilization Networks (LISNs). Similarly, another pair of LISNs is used to provide the *signal section* with a $12V$ DC power supply. The injection clamp (IC), which is mounted on the cable harness is driven by an RF chain comprising an RF source and a $100W$ RF amplifier. The magnitude of the bulk current is monitored by means of a current probe (CP) connected to a power meter. The optical signal generated by the transmitter, which is included in the test board (not shown in Fig. 6) is conveyed to an optical receiver by an optic fiber to be converted into a PWM voltage, which average value is proportional to the current sensor output voltage (V_{o}). Wanting to acquire the average value directly, the PWM signal is low-pass filtered then measured by a DC voltmeter. The RF source, the power meter and the DC voltmeter are controlled by the code hosted in a computer (not shown in Fig. 6), which implements the measurement procedure suggested in [5] for the BCI tests. In particular, the frequency of the CW interference generated by the RF source is set and its magnitude is increased step-by-step while monitoring the current sensor output voltage. The interference magnitude is increased as long as V_{o} exceeds the susceptibility criterion. i.e., $\Delta V_{\mathrm{o}} = 20\ mV$, or the RF current reaches $I_{\mathrm{RF-max}} = 100\ dB\mu A$ or the forward power of the RF amplifier reaches $P_{\mathrm{RF-max}} = 100\ W$. The measurement was repeated for a set of frequencies in the range $10 - 400\ MHz$ obtaining the results shown in Fig. 7. In this plot, crosses (x) point out that the susceptibility criterion was exceeded, circles (o) that the maximum available power of the RF amplifier was reached without exceeding the criterion, crosses (+) that the maximum RF current level was reached without exceeding the criterion.

Wanting to check whether the offset measured at the voltmeter was due the demodulation of the RFI in the current sense amplifier rather than in the ancillary circuits needed to acquire such a voltage, i.e., the microcontroller analog input or the voltage regulator, the BCI test was carried out with the amplifier output disconnected from the ADC input. Instead, the DC output voltage of a resistive divider included in the test board was provided to the microcontroller analog input. The voltage divider was connected to the voltage regulator output. In this preliminary measurement, the test board resulted immune to the RFI injected in the cable harness. The susceptibility criterion was never exceeded up to the maximum RF current magnitude $I_{\mathrm{RF-max}} = 100\ dB\mu A$.

On the basis of the BCI test results shown in Fig. 7, one can conclude that the current sensor is very susceptible to the RFI for frequencies above $200\ MHz$. This would mean that to pass the BCI test, in the DPI test the DUT should be immune to an incident power level greater than $52\ dBm$. This is unrealistic.

On the other end, at a closer look to the BCI test board, one can observe that the shunt resistor R_{sh} is inserted in the *power section* close to the load connector, the current sensor amplifier is a part of the *signal section*, which is far away. Therefore, the PCB traces connecting the shunt resistor to the amplifier inputs propagate the common mode interference but they also collect the electromagnetic field related to the RF current injected in the cable harness. Furthermore, at the radio frequency, the impedance of the shunt resistance is dominated by the stray inductance, meaning that the amplifier inputs are likely affected also by differential mode interference. Finally, it is worth mentioning that the offset voltage observed at the output of a differential amplifiers deals with the product of the common mode and the differential mode voltages applied to the inputs, as highlighted in [15].

IV. Proposed Method

This section presents a method to evaluate the incident power level the amplifier should be immune to in the DPI test to achieve the required immunity level in the BCI test. This allows one to select the current sensor amplifier on the basis of the DPI test results or to design the filter to be inserted between the shunt resistor and the amplifier in order to achieve higher immunity levels.

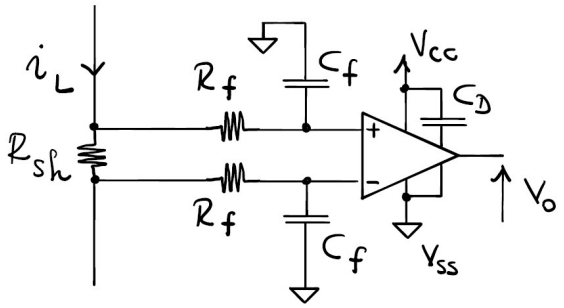


Fig. 9. HV current sensor including a first order common-mode/differential-mode filter.

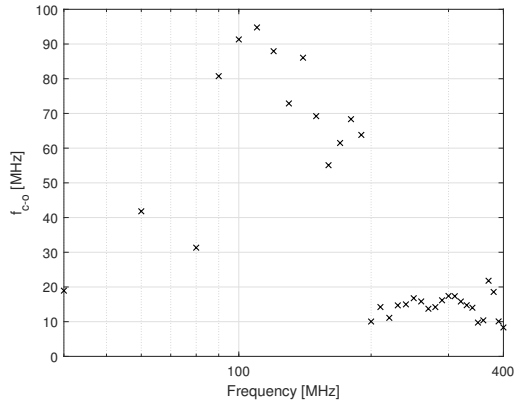


Fig. 10. Low-pass filter cut off frequencies.

As a first step, the DPI test is repeated with the RF interference applied to one of the amplifier input only. In this way, the amplifier is affected by the common mode and the differential mode interference, simultaneously. From this test the power level ($P_{\rm IN}$) causing the same output offset voltage experienced in the BCI tests is obtained. Fig. 8 shows such power levels versus frequency. As expected, the immunity level is much lower than that shown in Fig. 4, which resulted from applying the common mode interference only in the DPI test. Therefore, the power level the amplifier should be immune to in the DPI test, in order to obtain the desired immunity level in the BCI test are given by

$$P_{\rm IN,target,dBm} = P_{\rm IN,dBm} + \Delta_{\rm dB}, \tag{3}$$

where

$$\Delta_{\rm dB} = I_{\rm RF-max,dB\mu A} - I_{\rm RF-fail,dB\mu A}. \tag{4}$$

In our case, the target level for the bulk current is $I_{\rm RF-max} = 100\ dB\mu A$, therefore, the minimum RF power level to be applied to one of the amplifier inputs in the DPI test with the output offset voltage not exceeding the maximum value $\Delta V_{\rm o,max} = 20\ mV$ is that shown by the red circles in Fig. 8. Such an immunity level can be achieved by replacing the current sensor amplifier with another one, which is immune to the power level shown by the red circles in Fig. 8 or by inserting a low pass filter between the shunt resistance and the amplifier inputs, as it is shown in Fig. 9. Such a filter is effective in attenuating both the common mode and the differential mode as long as it is inserted close to the amplifier

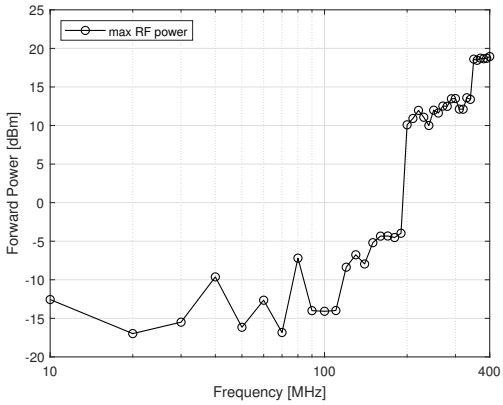


Fig. 11. DPI test results obtained with the low-pass filter inserted in the test board.

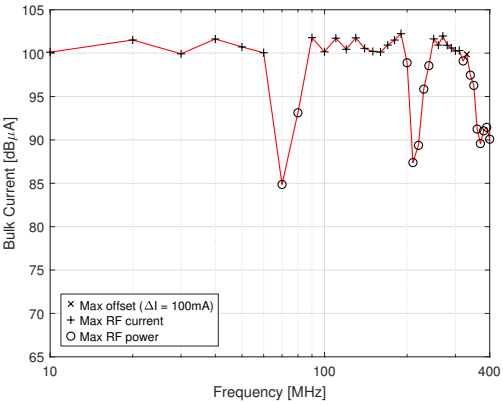


Fig. 12. BCI test results obtained with the low-pass filter inserted between the shunt resistor $R_{\rm sh}$ and the amplifier's inputs.

input terminals, so that stray inductances and capacitances are minimized. To this purpose, it is worth mentioning that the filter can be designed and validated referring to the DPI test board rather than the application one, which would require the complete module working in the BCI test set up.

V. Filter Design

A first order low pass filter like that shown in Fig. 9 is considered. Its attenuation, both for the common mode and the differential mode, can be written as

$$|H(f)| = \frac{1}{\sqrt{1+\left(\frac{f}{f_{\rm c-o}}\right)^2}}, \tag{5}$$

where $f_{\rm c-o}$, the cut-off frequency, is given by

$$f_{\rm c-o} = \frac{1}{2\pi R_{\rm f} C_{\rm f}}, \tag{6}$$

$R_{\rm f}$, $C_{\rm f}$ are the resistance and capacitance composing the filter. For $f >> f_{\rm c-o}$, (5) can be approximated as

$$|H(f)| \simeq \frac{f_{\rm c-o}}{f}, \tag{7}$$

thus the cut-off frequency that provided the desired attenuation at the generic frequency f' is given by

$$f_{\rm c-o} \simeq |H(f')|\, f'. \tag{8}$$

Fig. 10 shows the cut-off frequency $f_{\mathrm{c-o}}$ obtained by (8) for the frequency vector used for the BCI and the DPI tests (f'). The minimum value taken by $f_{\mathrm{c-o}}$ is the one that allows for having the attenuation needed all over the frequency range of interest. In Fig. 10 the minimum is $f_{\mathrm{c-o}} = 8\ MHz$ at $f' = 400\ MHz$. Therefore, a low pass filter with this cut-off frequency was designed. $R_{\mathrm{f}} = 200\Omega$, $C_{\mathrm{f}} = 100pF$ were selected, then inserted in the DPI test board, and the DPI test was repeated referring to the power level shown in Fig. 8 (red circles) obtaining the plot in Fig. 11. With the low-pass filter inserted in the test board, the amplifier never exceeded the susceptibility criterion, meaning the maximum output offset voltage $\Delta V_{\mathrm{o,max}} = 20\ mV$. Finally, the same filter was inserted in the BCI test board and the test was repeated obtaining the results shown in Fig. 12. Also in this case, the output voltage of the current sensor never exceeded the susceptibility criterion.

VI. Conclusions

This work has shown that not isolated HV current sensors used to monitor the current provided to power loads are highly affected by the RFI injected in the power cables. A method to investigate their susceptibility to the RFI at the component level with the purpose of obtaining the compliance at the module level has been proposed and its effectiveness validated experimentally.

References

[1] S. Ziegler, R. Woodward, H. Ho-Ching Iu, L. Borle, "Current Sensing Techniques: A Review," IEEE Sensor Journal, vol.9, no.4, pp. 354–376, 2009.

[2] AN-296276: Current sensing in motor drives, Allegro Microsystems, 2023.

[3] Z. Xin, Y. Yao, J. Kang, Q. Li, Z. Zhou, Y. Shi, "A Closed-Loop Compensated Rogowski Coil Current Sensor for Three-Phase Inverter," IEEE Trans. on Power Electronics, vol. 40, no. 1, pp. 2126–2138, 2025.

[4] AMC0x11D-Q1 datasheet, Dec. 2024. [Online]. Available: https://www.ti.com

[5] ISO 11452-4: Road vehicles – Component test methods for electrical disturbances from narrowband radiated electromagnetic energy, rev5, 2020.

[6] O. Aiello, P. Crovetti, F. Fiori, "Investigation on the susceptibility of hall-effect current sensors to EMI," in Proc. of IEEE International Symposium on Electromagnetic Compatibility (EMC-Europe), 2011, York, UK, pp. 368–372.

[7] P. Schroeter, F. Ballarin, F. Fiori, "Susceptibility to EMI of high side current sensors based on chopper OpAmps," in Proc. of 10th International Workshop on the Electromagnetic Compatibility of Integrated Circuits (EMC Compo), Edinburg, UK, pp. 115–118, 2015.

[8] D. Kircher, B. Deutschmann, H. Helldorff, "A Novel Method for Testing the Electromagnetic Immunity of the Short Circuit Protection Function of Smart Power Switches," Asia-Pacific International Symposium on Electromagnetic Compatibility (APEMC), Okinawa, Japan, pp. 661–664.

[9] T. Hartman, B. Have, J. Dijkstra, R. Grootjans, N. Moonen, F. Leferink, "Susceptibility of Static Energy Meters due to Amplifier Clipping Caused by a Rogowski Coil," IEEE Trans. on Electrom. Compat., vol. 64, no. 6, pp. 2024–2032, 2022.

[10] O. Aiello, F. Fiori, "A New MagFET-Based Integrated Current Sensor Highly Immune to EMI," Elsevier Microelectronics Reliability, vol. 53, Issue. 4, pp. 573–581, 2013.

[11] O. Aiello, F. Fiori, "A new mirroring circuit for power MOS current sensing highly immune to EMI," MDPI Sensor, vol. 13, Issue 2, pp. 1856–1871, 2013.

[12] M. Fishta, F. Fiori, "On the Robustness of Discrete-Time and Continuous-Time $\Sigma\Delta$ Modulators to Conducted RFI," IEEE Trans. on Electrom. Compat., vol. 66, no. 5, pp. 1515–1524, 2024.

[13] INA 240 datasheet, Dec. 2021. [Online]. Available: https://www.ti.com

[14] IEC 62132-4: Integrated Circuits, Measurement of Electromagnetic Immunity, 150 kHz - 1 GHz, IEC Standard, 2006.

[15] F. Fiori, "EMI-Induced Distortion of Baseband Signals in Current Feedback Instrumentation Amplifiers," IEEE Trans. on Electrom. Compat., vol. 60, no. 3, pp. 605–612, 2018.

[16] F. Fiori, "Susceptibility to Radio Frequency Interference of eGaN Power Switching Legs," in Proc. of IEEE Symposium on Electromagnetic Compatibility and Signal/Power Integrity (EMC+SIPI), Grand Rapids, MI, USA, pp. 548–553, 2023.